EFFECTS OF FLUID INERTIA AND TURBULENCE ON FORCE

COEFFICIENTS FOR SQUEEZE FILM DAMPERS*

Luis San Andrés and John M. Vance
Texas A&M University
College Station, Texas 77843

The effects of fluid inertia and turbulence on the force coefficients of squeeze film dampers are investigated analytically. Both the convective and the temporal terms are included in the analysis of inertia effects. The analysis of turbulence is based on friction coefficients currently found in the literature for Poiseuille flow.

The effect of fluid inertia on the magnitude of the radial direct inertia coefficient (i.e. to produce an apparent "added mass" at small eccentricity ratios, due to the temporal terms) is found to be completely reversed at large eccentricity ratios. The reversal is due entirely to the inclusion of the convective inertia terms in the analysis.

Turbulence is found to produce a large effect on the direct damping coefficient at high eccentricity ratios. For the long or sealed squeeze film damper at high eccentricity ratios, the damping prediction with turbulence included is an order of magnitude higher than the laminar solution.

NOMENCLATURE

a	= inner cylinder radius
$\overline{a}_r = -\varepsilon$	= dimensionless journal center radial acceleration
b	= outer cylinder radius
$\overline{C}_{rt}, \overline{C}_{tt}$	= dimensionless damping coefficients in (r,t) directions due to tangential velocity $\overline{V}_t$
C_{rt}, C_{tt}	= damping coefficients = $(\overline{C}_{rt}, \overline{C}_{tt}) * \mu kL/\delta^3$
$\overline{D}_{rr}, \overline{D}_{tr}$	= dimensionless inertia coefficients in (r,t) direction due to normal acceleration $\overline{a}_r$
D_{rr}, D_{tr}	= inertia coefficients = $(\overline{D}_{rr}, \overline{D}_{tr}) * \mu kL/\delta^3\omega$
e	= circular centered orbit radius
f_r, f_t	= dimensionless fluid film force in (r,t) direction

f_θ, f_ξ = inertial wall shear stress functions

$H = 1 + \varepsilon c\theta$: dimensionless film thickness

$h = b\delta H$ = film thickness

$I_{\theta\theta}$, $I_{\theta\xi}$, $I_{\xi\xi}$ = momentum integrals over the film thickness

k = geometry parameter = $(L/b)^2$ for short SFD assumption, 1 for others

k_θ, k_ξ = parameters depending on the nature of the flow

L = squeeze film damper length

p = pressure

$\bar{p} = p\delta^2/(k\omega\mu)$ = dimensionless pressure

q_θ, q_ξ = dimensionless local flow rates in (θ,ξ) direction

$Re = \omega\delta^2 b^2/\nu$ = squeeze Reynolds number

$Rep = \dfrac{Re}{\delta}\ [(q_\theta+H)^2 + (L/b\ \ q_\xi)^2]^{\frac{1}{2}}$ = Poiseuille flow Reynolds number

u = fluid relative velocity along lubricant film

u^* = absolute fluid velocity along lubricant film = $u+b\omega$

$\bar{u}$ = $u/b\omega$: dimensionless fluid velocity

$\bar{u}_m$ = $\displaystyle\int_0^1 \bar{u}d\eta$ = mean fluid velocity along lubricant film

v = fluid velocity across lubricant film

$\bar{v}$ = $v/b\delta\omega$ = dimensionless fluid velocity

$\bar{V}_t$ = ε = dimensionless journal center tangential velocity

w = fluid velocity in the axial direction

$\bar{w}$ = $w/L\omega$ = dimensionless axial velocity

$\bar{w}_m$ = $\displaystyle\int_0^1 \bar{w}d\eta$ = mean fluid velocity in axial direction

ω = frequency of damper motion

t = time

(x,y,z) = moving coordinate system

$(x,y,z)^*$ = fixed coordinate system

$\alpha_1, \alpha_2, \alpha_3$ = coefficients eventually depending on Re for turbulent motion

γ = $\partial H / \partial \theta$ = film thickness gradient along circumferential direction

Γ = $\Gamma(\overline{um}^2)$ = dimensionless inertia function for long SFD assumption

δ = $(b-a)/b$ = clearance ratio

ϵ = $e/b\delta$ = dimensionless circular orbit radius, eccentricity radius

(θ, η, ξ) = dimensionless coordinates = $(x/b, y/h, z/L)$

$\Delta\tau_{\theta\eta}, \Delta\tau_{\xi\eta}$ = wall shear stress difference in (θ, ξ) direction

ρ = fluid density

μ = fluid viscosity

ν = μ/ρ = kinematic viscosity

τ = $t\omega$ = dimensionless time

Subscripts:

o = inertialess or purely viscous

i = inertial

INTRODUCTION

Squeeze film dampers (SFD) are designed to have a stabilizing effect on the rotordynamics of turbomachinery. This has generally been accomplished by using the Reynolds effect in a thin oil film around a bearing to produce a predictable damping coefficient. The increase in size and speed of modern turbomachinery using light viscosity oils has brought the need to include fluid inertia effects in the design analysis. Sparked by the recent pioneering work of Tichy [1-4], researchers are now extending the lubrication theory into the range where the Reynolds (slow flow) assumption is no longer applicable.

At least for some simple geometries and motions, the fluid inertia effects have been shown to be quite significant.

To the rotordynamicist fluid film forces and dynamic coefficients are more important than velocity or pressure fields. Analytical [2,7] and numerical [5,6] approaches have been developed for calculating the damping and inertia coefficients, assuming motions of small amplitude α about an equilibrium point. In this case, it can be shown that the convective inertial terms may be neglected in the equations of motion, since they are of order α^2 while the temporal terms are of order α. In all these analyses, the trend of the damping and inertia coefficients is to increase as the static eccentricity ratio increases, a fact that has been shown to be true in practice.

However, for large excursions of the journal center about its centered position the full inertial term should be retained in the momentum equations. The temptation to neglect convective terms in order to simplify and linearize the problem is no longer justifiable even for very simple cases such as the long or short bearing solutions. For example, reference [9] recently presented numerical calculations for the dynamic coefficients of an SFD performing circular orbits (CCO) about the center of the bearing housing. Using the same approach as in [5], the convective inertia effects were neglected, so the coefficients have the characteristic form described above. This behavior of the fluid film forces will be shown to be in error even for moderate eccentricities and totally incorrect at large orbit amplitudes. Furthermore, in reference [9] the direct damping and inertia coefficients for the cavitated SFD were found to be one half the value of the full film case and independent of the inertia parameters of the fluid. This appears unreasonable since if cavitation is allowed, the extent of the region where the film is broken will be influenced by the magnitude of the inertial forces. Our purpose in the present analysis will be to determine the dynamic coefficients taking into account the full inertial terms for simple geometries in order to understand better the action of viscous and inertial forces in an SFD.

The inclusion of inertia complicates the problem in a SFD, and turbulence effects make the problem even more involved. Unlike the journal bearing case where a considerable amount of analytical and experimental work has been done, turbulence in squeeze film dampers remains rather obscure due to the lack of experimental data or a good understanding of the mechanics of squeezing flows. Nelson [11] used the empirical friction coefficient for pure Poiseuille flows in an attempt to include turbulent effects for the long SFD case. No satisfactory results were obtained since the fluid apparent viscocity was used to calculate the empirical friction factor for the flow.

Tichy [4] suggests that turbulent flow in SFD's will occur at higher Reynolds numbers than for Poiseuille flows, i.e. Rep > 2000. This assertion seems reasonable since the velocity field in a SFD is constantly changing and adjusts itself to the normal motion of the boundary, thus making the flow more stable. It also seems reasonable that transition from laminar to turbulent regions should be smooth in order to satisfy continuity of the flow. All these considerations make the problem more untractable and point out the urgent need of experimental data. In the mean-time, it will prove helpful to use the empirical correlations currently found in the literature and thus obtain upper bounds for the forces and dynamic coefficients when turbulence is present in the flow.

STATEMENT OF THE PROBLEM

Figure 1 shows the geometry of the SFD system. The equations of motion for the flow in the annular region between a whirling nonrotating inner cylinder and its bearing housing are stated in a moving coordinate frame. Appendix A contains the details of the integration of the motion equations across the lubricant film, to finally obtain in dimensionless form:

$$\text{Re} \left\{ \frac{\partial}{\partial \theta} I_{\theta\theta} + \frac{\partial}{\partial \xi} I_{\theta\xi} \right\} = -\text{Hk} \frac{\partial \bar{p}}{\partial \theta} + \Delta \tau_{\theta\eta} \tag{1}$$

$$\text{Re} \left\{ \frac{\partial}{\partial \theta} I_{\theta \xi} + \frac{\partial}{\partial \xi} I_{\xi \xi} \right\} = -\text{Hk} \ (b/L)^2 \ \frac{\partial \bar{p}}{\partial \xi} + \Delta \tau_{\xi \eta} \tag{2}$$

$$\frac{\partial}{\partial \theta} q_\theta + \frac{\partial}{\partial \xi} q_\xi = 0 \tag{3}$$

This system of equations must be solved with appropriate boundary conditions for the flow rates (q_θ, q_ξ) and the pressure $\bar{p}$. Analytical solutions to the problem are extremely difficult since the exact form of the wall shear stress difference ($\Delta \tau_{\theta \eta}$, $\Delta \tau_{\xi \eta}$) is unknown and some assumption regarding their functional form becomes necessary. Presumably, the problem may be solved numerically on a computer with its full tridimensional complexity, but such an effort may prove to be unnecessarily costly or even impractical.

As a first approximation to a practical solution of the problem, we assume that for the laminar region, and even in the presence of turbulent effects, the shear stresses at the walls may be written as:

$$\Delta \tau_{\theta \eta} = -k_\theta \ \frac{(q_\theta + H)}{H^2} + \text{Re} \ f_\theta \tag{4a}$$

$$\Delta \tau_{\xi \eta} = -k_\xi \ \frac{q_\xi}{H^2} + \text{Re} \ f_\xi \tag{4b}$$

The approximate form of the functions k_θ, k_ξ, f_θ and f_ξ will be discussed later in the analysis. Note also that in equations (4) we have included an explicit contribution of inertia to the wall shear stress difference.

Once a solution to the system of equations (1) to (3) has been obtained the fluid film forces acting on the inner cylinder are calculated by integration of the pressure distribution over the flow region. For rotordynamics applications, the forces are expressed in terms of damping and inertia coefficients. Let (f_r, f_t) be the radial (along the centerline of both cylinders) and tangential dimensionless fluid film forces, and given by:

$$f_r = \int_R \bar{p} \cos \theta \ dR = - \bar{C}_{rt} \ \bar{V}_t - \bar{D}_{rr} \ \bar{a}_r \tag{5a}$$

$$f_t = \int_R \bar{p} \sin \theta \ dR = - \bar{C}_{tt} \ \bar{V}_t - \bar{D}_{tr} \ \bar{a}_r \tag{5b}$$

$$R = \{ 0 \le \theta \le 2\pi , \ 0 \le \xi \le 1 \}$$

In equations (5), $\bar{V}_t$, $\bar{a}_r$ are the dimensionless journal center tangential velocity and radial acceleration, respectively; and ($\bar{C}_{rt}$, $\bar{C}_{tt}$), ($\bar{D}_{rr}$, $\bar{D}_{tr}$) are the dimensionless damping and inertia coefficients. The dimensional counterparts of these coefficients are given by the relations:

$$C_{ij} = \frac{\mu k L}{\delta^3} \ \bar{C}_{ij} \ , \quad D_{ij} = \frac{\mu k L}{\delta^3 \omega} \ \bar{D}_{ij} \tag{6}$$

Our interest is to obtain approximate solutions to the uncavitated case, and present the dynamic coefficients with inertia and turbulence effects accounted for in the flow. This is a necessary step preliminary to any more refined analysis, since it will contribute to a better understanding of the problem. We will treat the laminar and turbulent solutions for the long and short SFD's separately. No cavitation is considered in the flow region. This last assumption is unrealistic for some cases, but permits us to do a first treatment of the fluid film forces with inertia and turbulence included, and will be accurate for high supply pressures. Furthermore, the direct effects of fluid inertia and turbulence will be isolated from the indirect effect caused by changes in the region of cavitation.

LAMINAR FLOW SOLUTIONS

Long Bearing Assumption

In this section we assume that the cylinders are infinite in extent, or that very tight end seals are placed at the ends of the SFD, or that the axial flow q_ξ is negligible. We are left with the equation:

$$q_\theta = \bar{u}_m H \tag{7}$$

$$\frac{\partial \bar{p}_o}{\partial \theta} = \frac{-k_\theta}{H^3} (q_\theta + H) \tag{8}$$

$$\frac{\partial \bar{p}_i}{\partial \theta} = \frac{\gamma}{35H} [-7 + 35\alpha_1 \bar{u}_m^2] + \frac{f_\theta}{H} \tag{9a}$$

$$\bar{p} = \bar{p}_o + Re\ \bar{p}_i$$

Here we have divided the pressure into two parts so that $\bar{p}_i$ contains explicitly the influence of inertia.

For small Reynolds numbers, Re<1, Brindley [7] and the first author [10] have found that $k_\theta = 12$ as in the usual lubrication approximation, and that the inertial pressure gradient is given by:

$$\frac{\partial \bar{p}_i}{\partial \theta} = \frac{\gamma}{35H} [-6 + 6\bar{u}_m + 54\bar{u}_m^2] \tag{9b}$$

For large Reynolds numbers, assuming that the flow remains stable and laminar, the inviscid pressure gradient is given as:

$$\frac{\partial \bar{p}_i}{\partial \theta} = \frac{\gamma}{H} \bar{u}_m^2 \tag{9c}$$

Equation (9c) is different from the result presented by Tichy in [4], apparently due to an error in the boundary conditions used for the inviscid flow region.

For both extreme values of the inertial parameter Re, the dimensionless flow rate q_θ is unaffected by inertia and is equal to:

$$q_\theta = \frac{2(\varepsilon^2 - 1)}{(2 + \varepsilon^2)} \tag{10}$$

In order to make a quantitative comparison of equations (9a-9c) we let:

$$\Gamma = \frac{H}{\gamma} \frac{\partial \overline{P}_i}{\partial \theta} = \Gamma(\overline{u}_m{}^2) \tag{11}$$

be a function that indicates the magnitude of the inertia term in the pressure equation.

Figure 2 shows equations (9a-9c); curve A represents (9a) with $f_\theta = 0$, $\alpha_1 = 1.2$, curves B & C, equation (9b-c), respectively.

A brief look at figure 2 shows the surprisingly similar behavior of the flow for the large range of Re considered. The actual value of Γ for moderate Reynolds numbers will lie between curves A and B; curve F shows the best fitting line between the A and B curves from which we select the inertial contribution to the wall shear stress difference as:

$$f_\theta = \frac{4}{35} \gamma \frac{q_\theta{}^2}{H^2} \tag{12}$$

Thus, we assume that for moderate Reynolds numbers, the wall shear stress difference is approximately given by:

$$\Delta \tau_{\theta\eta} = -12 \frac{(q_\theta + H)}{H^2} + Re \frac{4}{35} \gamma \frac{q_\theta{}^2}{H^2} \tag{13}$$

With these considerations, the pressure field for the flow can be determined, and from this, the dynamic coefficients. As previously stated, only the uncavitated SFD is treated here so that the effect of inertia on the fluid film forces can be clearly isolated. Otherwise, the extent of the cavitated region is dependent on the Reynolds number and the dynamic coefficients must be determined numerically for each change in the inertia parameter.

Integration of equations (8) and (9), subject to the continuity condition for the pressure field, is relatively easy and is given in [8]. The dynamic coefficient for the long SFD with laminar flow come to be:

$$\overline{C}_{rt} = \overline{D}_{tr} = 0 \ , \quad \overline{C}_{tt} = \frac{24\pi}{(2 + \varepsilon^2)(1 - \varepsilon^2)^{\frac{1}{2}}} \tag{14}$$

Note that the direct damping coefficient $\overline{C}_{tt}$ is the same as in the inertialess solution. Analytical expressions for the direct inertia coefficient $\overline{D}_{rr}$ are given in Table I. Figure 3 shows a comparison of this coefficient for the different cases considered. The behavior of the inertia coefficient $\overline{D}_{rr}$ divided by Re is surprisingly similar for the large range of Reynolds number considered. The largest

difference occurs at small and large eccentricities but is never more than 20%, (between Re=0 and Re=∞). The rapid decrease of the inertia coefficient as the eccentricity ratio grows larger appears to contradict the recent results presented in [9]. The reason for the discrepancy is that in the MTI study only temporal acceleration effects were accounted for in the equation of motion while here both the convective and temporal inertia terms are retained. The upper dashed curve in figure 3 shows the inertia coefficient when only the temporal effects are included. The coefficient grows rapidly and even goes to infinity as the orbit size approaches the radial clearance.

Short Bearing Assumption

In this section we assume that the SFD has small L/D ratios, the ends are open to the atmosphere, and for simplicity we also assume that no high externally induced axial flow is present in the damper. The reason for the latter assumption is to avoid pressure boundary conditions which would require the explicit presence of the inertial parameter Re. As is current practice for the short journal bearing analysis, the circumferential flow is assumed to be negligible. We set $k=(L/b)^2$ in eqs. (1) to (3) and get the following set of equations:

$$q_\theta = -H \tag{15}$$

$$\frac{\partial q_\xi}{\partial \xi} = \gamma \tag{16}$$

$$\frac{H \, \partial \bar{p}_o}{\partial \xi} = -12 \, \frac{q_\xi}{H^2} \tag{17}$$

$$\frac{H \, \partial \bar{p}_i}{\partial \xi} = f_\xi + \frac{\partial q_\xi}{\partial \theta} - \frac{\alpha_3}{H} \frac{\partial}{\partial \xi} (q_\xi^{\,2}) \tag{18a}$$

The axial inertial pressure gradient obtained for small Re using a regular perturbation solution in Re is given by Tichy (3) as:

$$\frac{H \, \partial \bar{p}_i}{\partial \xi} = 1.2 \, \frac{\partial q_\xi}{\partial \theta} - \frac{51}{35H} \frac{\partial}{\partial \xi} (q_\xi^{\,2}) \tag{18b}$$

Assuming the flow remains stable and laminar, for large Re the inviscid pressure gradient is given by:

$$\frac{H \, \partial \bar{p}_i}{\partial \xi} = \frac{\partial q_\xi}{\partial \theta} - \frac{1}{H} \frac{\partial}{\partial \xi} (q_\xi^{\,2}) \tag{18c}$$

From a quantitative comparison of equation (18a-c), for moderate Reynolds numbers we select the inertial contribution to the wall shear stress difference to be:

$$f_\xi = -\frac{2}{35H} \frac{\partial}{\partial \xi} (q_\xi^{\,2}) + \frac{1}{10} \frac{\partial q_\xi}{\partial \theta} \tag{19}$$

372

Thus, we assume that the wall shear stress difference for the short SFD approximation is given by:

$$\Delta \tau_{\xi\eta} = - k_\xi \frac{q_\xi}{H^2} - \frac{2}{35H} \frac{\partial}{\partial \xi} (q_\xi^2) + \frac{1}{10} \frac{\partial q_\xi}{\partial \theta}$$

(20)

With these considerations, equations (17) and (18a-c) are integrated to obtain the pressure field. For the full film assumption, the dynamic coefficients come to be:

$$\overline{C}_{rt} = \overline{D}_{tr} = 0 \ , \quad \overline{C}_{tt} = \frac{\pi}{(1-\varepsilon^2)^{3/2}}$$

(21)

Note that the direct damping coefficient $\overline{C}_{tt}$ is the same as in the inertialess solution. Analytical expressions for the direct inertia coefficient $\overline{D}_{rr}$ are given in Table II. For the different cases considered, figure 4 shows the inertia coefficient $\overline{D}_{rr}$ divided by Re as a function of the eccentricity. As in the long SFD case, the form of the inertia coefficient is surprisingly similar for the large range of squeeze Reynolds numbers considered. Note the tremendous influence that the convective inertial terms have on the coefficient when compared to the dashed curve which is based only in the inclusion of temporal effects on the equation of motion. Thus, analyses based on small perturbation about an equilibrium point are in large error compared to the exact solution, if the orbit is large.

TURBULENT FLOW SOLUTIONS

The inclusion of turbulence effects into the flow complicates the problem enormously. Although the mechanism of turbulence for fully developed Couette and Poiseuille flows has been studied extensively, both analytically and experimentally, and many contributions to the analysis of flow in narrow channels have been given in the past years; the mechanics of squeezing flows are far more complicated. The subject still remains obscure due to the complete absence of theoretical-empirical formulation and the lack of experimental results.

Undaunted, we assume that the coefficients k_θ & k_ξ to be used in turbulent flow in a SFD are given by:

$$k_\xi = k_\theta = 12 + 0.005 \ \text{Rep}$$

(22)

where

$$\text{Rep} = \frac{Re}{\delta} \ [(q_\theta+H)^2 + (L/b)^2 \ q_\xi^2]^{\frac{1}{2}}$$

(23)

is the Poiseuille Reynolds number currently found in the literature.

Relation (22) was obtained as the best fitting curve between the experimental correlation given by Hirs (12) and the analytical results based on the mixing length theory given by Elrod and Ng (13). Here we have assumed that the transition from the laminar to turbulent regions in a SFD must be smooth in order to insure continuity of the flow.

373

The assumed expressions may be far away from the actual expressions which should be obtained from experimental results. However, we have chosen them in the absence of better empirical formulations, and the results obtained will prove to be upper bounds of the actual forces and dynamic coefficients.

Long Journal-Bearing Assumption

As in section 3.a, the axial flow is neglected and the pressure gradient field is given by:

$$\frac{\partial \bar{p}}{\partial \theta} = -(12 + 0.005 \frac{Re}{\delta} 1H + q_\theta 1) \frac{(H+q_\theta)}{H^3} + \frac{Re}{35} \frac{\gamma}{H} [-7+46 \frac{q_\theta^2}{H^2}] \tag{24}$$

$$q_\theta = q_\theta (\varepsilon, Re, \delta) \tag{25}$$

Note that we have assumed that f_θ given in (12) prevails even in the turbulent regime. A very simple computer code was written to obtain the pressure field. Using numerical integration, the dynamic coefficients were calculated for an uncavitated SFD with a clearance ratio $\delta = 0.001$.

Figure 5 shows the direct damping coefficient $\bar{C}_{tt}$ as a function of the eccentricity ratio for different Re, and figure 6 depicts the same coefficient as a function of the Reynolds number for different orbit radius ε. From the figures it is evident that turbulence has a large effect on the damping coefficient, and consequently on the tangential force. This is due to the increase in the apparent viscocity of the fluid as the inertia parameter grows.

Figure 7 shows the direct inertia coefficient $\bar{D}_{rr}/Re$ for various orbit radius, the pattern of the curves is the same as in figure 3 for moderate Reynolds numbers. It is clearly seen that the effect of turbulence is to increase the coefficient, especially at large whirling orbits, this is due to the increase in flow rate q_θ as ε grows in order to satisfy continuity of the pressure field.

A comparison of the results given in figures 5 and 7 shows that the ratio $\bar{D}_{rr}/\bar{C}_{tt}$ is less than 1/10 for all eccentricities and Reynolds numbers considered, this may be an important result since it implies that the tangential force will be larger than the purely inertial radial force.

Short Journal Bearing Assumption

For the short SFD assumption, the axial pressure gradient equation comes to be:

$$\frac{\partial \bar{p}}{\partial \xi} = -(12+0.005\frac{Re}{\delta} (L/b) 1q\varepsilon 1) \frac{q_\xi}{H^3} + \frac{Re}{H} [\frac{11}{10} \frac{\partial q_\xi}{\partial \theta} - \frac{44}{35H} \frac{\partial}{\partial \xi} q_\xi^2] \tag{26}$$

$$\frac{\partial q_\xi}{\partial \xi} = -\gamma \tag{27}$$

Assuming that there is no high axial flow externally induced into the SFD, the flow q_ξ remains unchanged from the inertialess solution. Equations (26) and (27) are amenable of closed form integration, the details of the same are omitted for

brevity; it is found that the direct inertia coefficient $\bar{D}_{rr}$ is the same as given in equation (2) of Table 2.

Figure 8 shows the direct damping coefficient $\bar{C}_{tt}$ as a function of the eccentricity ratio for different values of the squeeze Reynolds number Re, and figure 9 shows the same coefficient as a function of Re for various values of the orbit radius ε. All calculations were made for an uncavitated SFD with a clearance ratio of δ=0.001, and a L/D ratio equal to 0.25. From the figures a significant influence of turbulence on the damping coefficient is seen. As expected, the larger the Reynolds number, the larger the dynamic coefficient and consequently the tangential force increases proportionally. Once again, this effect is due to the increase in the apparent viscocity of the fluid as the inertia parameter grows.

SUMMARY

The present paper has considered the influence of inertia and turbulence on the flow in the annular region between a whirling damper journal, describing circular centered orbits, and its bearing. After an analysis of the fluid-flow equation for the problem, the usual assumptions considering the length of the SFD are made to obtain the classical long and short journal bearing approximations.

The region of flow was assumed to be continuous, i.e. no cavitation was allowed in the fluid. This allowed a clear analysis of the effect of inertia and turbulence on the fluid film forces and the dynamic coefficients. The laminar solution showed the importance of the inclusion of convective inertia terms in the equations of motion. The resulting reversal of the "added mass effect" makes it clear that numerical or analytical approaches that calculate the dynamic coefficients for large motion amplitudes in base to small perturbations about an equilibrium point may be largely in error.

In the absence of empirical coefficients for the turbulent motion in squeezing flows, a friction coefficient based on the Poiseuille analysis of Hirs and Elrod and Ng was used. This may be modified by experimental results in the future, since the transition from laminar to turbulent motion may turn out to appear at larger Reynolds numbers than here considered. As suggested in reference (4), the values here presented should be considered as upper bounds for the actual dynamic coefficients and as qualitative indicators of the influence of turbulence on the flow. If these bounds are even approached by the real case, turbulence will be found to have a large effect on the direct damping coefficient for squeeze film dampers.

The present analysis should prove to be stepping stones for future developments that will consider SFD's of finite extent and also the influence of inertia in the boundary conditions of the flow.

REFERENCES

1. Modest, M. F., and J. A. Tichy, "Squeeze Film Flow in Arbitrarily Shaped Journal Bearings Subject to Oscillations," Journal of Lubrication Technology, July 1978, pp. 323-329.

2. J. A. Tichy, "Effects of Fluid Inertia and Viscoelasticity on Squeeze Film Bearing forces," ASLE Transactions, Vol. 25, January 1982, pp. 125-132.

3. J. A. Tichy, "A Simple Low Deborah Number Model for Unsteady Hydrodynamic Lubrication, Including Fluid Inertia," Journal of Rheology, Vol. 24, 1980, pp. 829-845.

4. J. A. Tichy, "The Effect of Fluid Inertia in Squeeze Film Damper Bearings: A Heuristic and Physical Description," ASME paper 83-GT-177.

5. Reinhardt, E. and Lund , J. W., "The Influence of Fluid Inertia on the Dynamic Properties of Journal Bearings," Journal of Lubrication Technology, April 1975, pp. 159-175.

6. Szeri, A. Z., A. A. Raimondi, A. Giron-Duarte, "Linear Force Coefficients for Squeeze Film Dampers," Journal of Lubrication Technology, July 1983, pp. 326-334.

7. Brindley, J., L. Elliott, J. T. McKay, "Flow in a Whirling Rotor Bearing," Journal of Applied Mechanics, December 1979, Vol. 46, pp. 767-771.

8. Szeri, A. Z., "Tribology: Friction, Lubrication and Wear," McGraw-Hill Co., N.Y., 1980, pp. 40.

9. Lund, J. W., A. J. Smalley, J. A. Tecza, J. F. Walton, "Squeeze Film Damper Technology: Part 1-Prediction of Finite Length Damper Performance," ASME Paper 83-GT-247.

10. San Andres, A., "Flow in a Journal Bearing Subject to Arbitrary Motions," Internal Report, Turbomachinery Labs, Mechanical Engineering Dept., Texas A&M University, December 1983.

11. Nelson, C., "The Effect of Turbulence and Fluid Inertia on a Squeeze Film Damper," AIAA/SAE/ASME, 16th Joint Propulsion Conference, June 30-July 2, 1980.

12. Hirs, G. G., "A Bulk Flow Theory for Turbulence in Lubricant Films," ASME Journal of Lubrication Technology, April 1973, pp. 137-146.

13. Elrod, H. G., C. W. Ng, "A Theory for Turbulent Fluid Films and its Applications to Bearings," ASME Journal of Lubrication Technology, July 1967, pp. 346-362.

TABLE I. Direct Inertia Coefficient $\overline{D}_{rr}$ for the
Long Squeeze Film Damper

Re	$\overline{D}_{rr}/Re$	
small Re<<1	$\frac{12}{35}\pi\ [\Gamma_2(1+2\beta b)\ +\ 9\Gamma_1]$	(1.2)
large Re$\rightarrow\infty$	$2\pi\Gamma_1$	(1.3)
moderate R_e $f_\theta=0$	$\frac{14}{35}\pi\ [\Gamma_2\ +\ 6\Gamma_1]$	(1.4)
moderate R_e f_θ from eqn. (12)	$\frac{14}{35}\pi\ [\Gamma_2\ +\ 6.5714285\ \Gamma_1]$	(1.5)

Definitions:

$$\beta = (1-\epsilon^2)^{\frac{1}{2}}\ ,\quad b = (2+\epsilon^2)^{-1} \tag{1.1}$$

$$\Gamma_1 = 2\beta b^2\ ,\quad \Gamma_2 = (\beta-1)/\epsilon^2$$

For temporal effects only:

$$D_{rr}/Re\ =\ \frac{-24}{10}\pi\ \Gamma_2 \tag{1.6}$$

TABLE II.   Direct Inertia Coefficient $\overline{D}_{rr}$

for the Short Squeeze Film Damper

$$\overline{D}_{rr}/Re = -\Gamma \, [C_1 + C_2 \, (\beta-1)] \qquad (2.1)$$

Re	C_1	C_2	
small Re<<1	1.2	102/35	(2.3)
large Re>>1	1.0	2.0	(2.4)
moderate R_e $f_\xi=0$	1.0	2.4	(2.5)
moderate R_e f_ξ from eqn. (19)	1.1	2(1+2/35)	(2.6)

Definitions:

$$(2.1) \qquad \beta = (1-\epsilon^2)^{\frac{1}{2}} \; , \quad \Gamma = \frac{\pi(\beta-1)}{6\beta\epsilon^2} \qquad (2.2)$$

Temporal Effects Only:

$$C_1 = 1.2 \; , \quad C_2 = 0 \qquad (2.7)$$

APPENDIX A

Coordinate System and Equations of Motion

Consider two circular cylinders of radii a and b (>a) and assume that the center of the smaller cylinder rotates with constant angular velocity ω in a circle of radius e about the center of the larger one. The condition that the cylinders do not touch is

$$0 \leq \varepsilon < 1 \qquad\qquad\qquad (A.1)$$

where $\delta = \dfrac{b-a}{a} \ll 1$, $\varepsilon = \dfrac{e}{(b-a)}$ $\qquad\qquad (A.2)$

Here δ and ε are the clearance and eccentricity ratios, respectively.

The first characteristic of the geometry of lubricant films that permits simplicication of the problem is that the thickness of the lubricant film, h, is very small compared to its length or to its radius of curvature. As consequences of this the following assumptions are made (8).

1) The effects of the curvature of the film are negligible.
2) The variation of the pressure across the film is small and may be neglected.
3) The rate of change of any velocity component along the film is small when compared to the rate of change of this same velocity component across the film and can be neglected.

In accordance with assumption (1), we can prescribe a fixed orthogonal cartesian coordinate frame $\{x_i^*\}_{i=1}^{3}$ in the plane of the lubricant film. See figure 1, where the y* axis is in the direction of the minimum film dimension. A moving orthogonal coordinate frame $\{x_i\}_{i=1}^{3}$ translating with velocity T=bω with respect to $\{x_i^*\}_{i=1}^{3}$ and its x axis perpendicular to the line joining the centers of both cylinders is introduced, and it can be shown that the flow will be steady to an observer moving with the $\{x_i\}_{i=1}^{3}$ frame.

The following dimensionless coordinates are introduced:

$$\theta = \frac{x}{b} \ , \quad \xi = \frac{z}{L} \ , \quad \eta = \frac{y}{h} \ , \quad \tau = t\omega \qquad\qquad (A.3)$$

where h = bδH(θ), H(θ) = 1 + $\varepsilon\cos\theta$ $\qquad\qquad\qquad (A.4)$

is the lubricant film thickness at location θ.

Dimensionless velocity components in the two coordinate frames are defined as

$$\overline{u}^* = \frac{u^*}{b\omega} \ , \ \overline{v}^* = \frac{v}{\delta b\omega} = \overline{v}, \ \overline{w}^* = \frac{w^*}{L\omega} = \overline{w}, \ \overline{u} = \frac{u}{b\omega} \qquad (A.5)$$

$$\overline{u}^* = \overline{u} + 1$$

The pressure and the shear stresses are made dimensionless according to

379

$$\bar{p} = \frac{(p-pa)\delta^2}{\omega\nu/\rho} k^{-1}, \quad \tau_{\theta\eta} = \frac{\tau_{xy}}{\omega\mu/\delta}, \quad \tau_{\xi\eta} = \frac{\tau_{zy}}{\omega\mu/\delta} \ (b/L) \tag{A.6}$$

and k=1 for long bearing assumption

$$k = (L/b)^2 \text{ for short bearing assumption} \tag{A.7}$$

With these considerations, the momentum and continuity equations for the tridimensional flow, expressed in the moving coordinate system are

$$\mathrm{Re} \left\{ \frac{\partial \bar{u}^2}{\partial\theta} + \frac{1}{H}\frac{\partial}{\partial\eta} [\overline{uv}-\eta\gamma\bar{u}^2] + \frac{\gamma\bar{u}^2}{H} + \frac{\partial}{\partial\xi} (\overline{uw}) \right\} = -k \frac{\partial\bar{p}}{\partial\theta} + \frac{1}{H}\frac{\partial}{\partial\eta} \tau_{\theta\eta} \tag{A.8}$$

$$\mathrm{Re} \left\{ \frac{\partial \bar{w}^2}{\partial\xi} + \frac{1}{H}\frac{\partial}{\partial\eta} [\overline{wv}-\eta\gamma\overline{wu}] + \frac{\gamma\bar{w}^2}{H} + \frac{\partial}{\partial\theta} (\overline{uw}) \right\} = -k \ (\tfrac{b}{L})^2 \frac{\partial\bar{p}}{\partial\xi} + \frac{1}{H}\frac{\partial}{\partial\eta} \tau_{\xi\eta} \tag{A.9}$$

$$\frac{\partial\bar{u}}{\partial\theta} + \frac{1}{H}\frac{\partial}{\partial\eta} [\bar{v}-\eta\gamma\bar{u}] + \frac{\gamma\bar{u}}{H} + \frac{\partial\bar{w}}{\partial\xi} = 0 \tag{A.10}$$

where $\gamma = \partial H/\partial\theta$ and

$$\mathrm{Re} = \frac{\omega\delta^2}{\nu} b^2 \tag{A.11}$$

is the squeeze Reynolds number.

The boundary conditions appropriate for the flow are

at η=0 $\bar{u}$=-1, $\bar{v}$=$\bar{w}$=0

η=1 $\bar{u}$=-1, $\bar{v}$=-γ, $\bar{w}$=0 $\qquad$ (A.12)

(Note that we have neglected the velocity component due to the motion of the surface η=1 in the θ-direction since it is of order δ).

The pressure must satisfy appropriate conditions at the ends of the SFD and must be single-valued and periodic in the circumferential direction, i.e.

$$\oint \frac{\partial\bar{p}}{\partial\theta} \, d\theta = 0 \tag{A.13}$$

Equations (A.8) to (A.10) are integrated across the film to obtain

$$\mathrm{Re} \left\{ \frac{\partial}{\partial\theta} I_{\theta\theta} + \frac{\partial}{\partial\xi} I_{\theta\xi} \right\} = -kH \frac{\partial\bar{p}}{\partial\theta} + \Delta\tau_{\theta\eta} \tag{A.14}$$

$$\mathrm{Re} \left\{ \frac{\partial}{\partial\theta} I_{\theta\xi} + \frac{\partial}{\partial\xi} I_{\xi\xi} \right\} = -kH \ (b/L)^2 \frac{\partial\bar{p}}{\partial\xi} + \Delta\tau_{\xi\eta} \tag{A.15}$$

$$\frac{\partial}{\partial\theta} q_\theta + \frac{\partial}{\partial\xi} q_\xi = 0 \tag{A.16}$$

where q_θ and q_ξ are the dimensionless local flow rates in the θ and ξ directions,

$$q_\theta = H \int_0^1 \bar{u}\,d\eta = H\,\bar{u}_m \qquad \text{(A.17a)}$$

$$q_\xi = H \int_0^1 \bar{w}\,d\eta = H\,\bar{w}_m \qquad \text{(A.17b)}$$

and the Iij's are defined as:

$$Iij = H \int_0^1 \bar{u}_i\,\bar{u}_j\,d_\eta \qquad \text{(A.18)}$$

To proceed, further assumptions about the velocity distribution should be made. To this end we assume that the shape of the velocity field is not greatly affected by inertia, and we let the velocity momentum integrals in (A.18) be given by

$$I_{\theta\theta} = \alpha_1\,q_\theta^2/H + 0.4\,q_\theta + 0.2\,H$$

$$I_{\theta\xi} = \alpha_2\,q_\theta q_\xi/H + 0.2\,q_\xi \qquad \text{(A.19)}$$

$$I_{\xi\xi} = \alpha_3\,q_\xi^2/H$$

For the type of flow considered, the range of variation of the coefficients $\{\alpha_i\}_{i=1}^3$ is between 1.2 and 1.0 for small Reynolds numbers and large Reynolds numbers, respectively; thus it may be assumed that averaged values will suffice to obtain meaningful results.
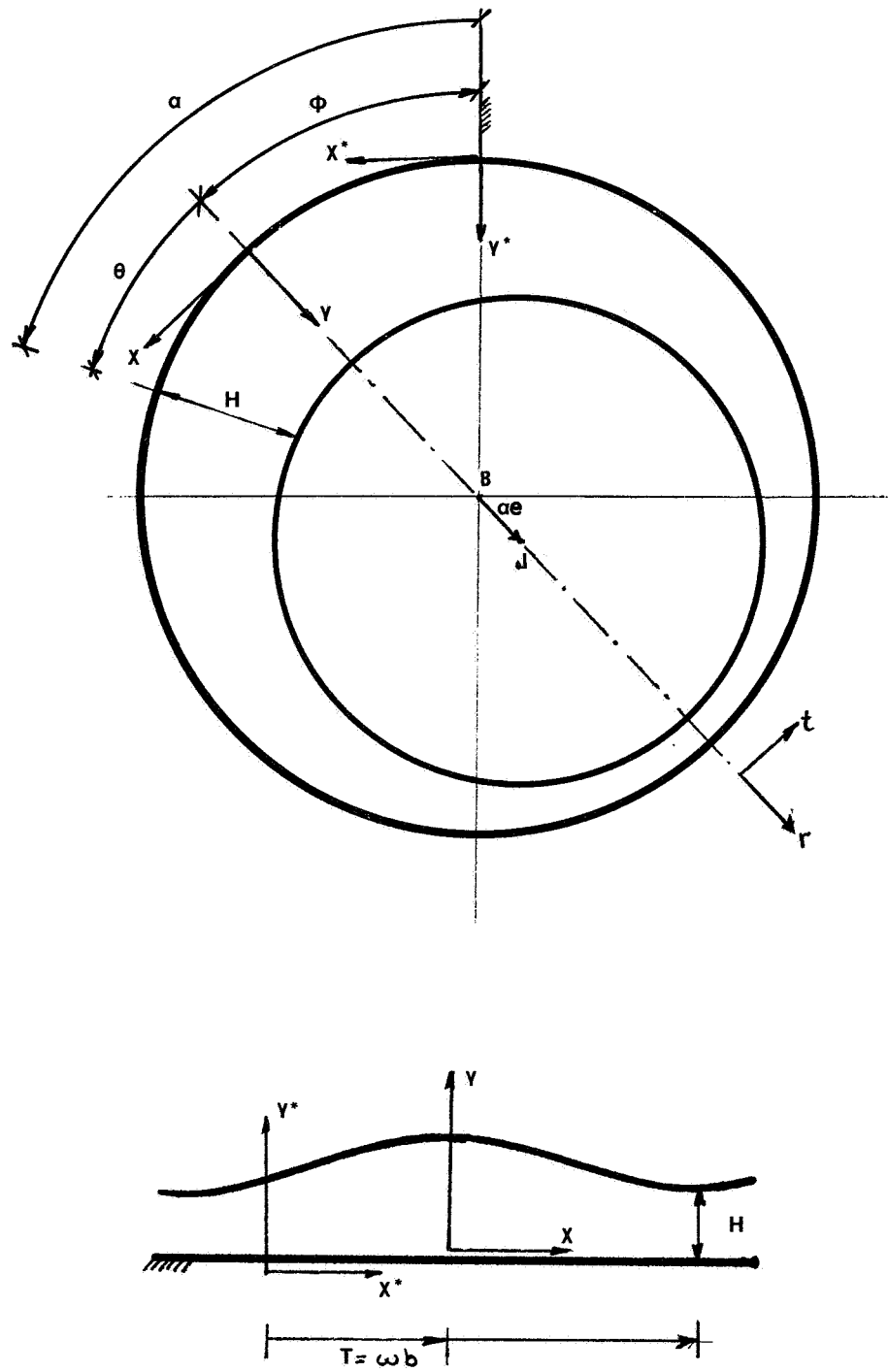
Figure 1. - Squeeze film damper geometry and coordinate systems.
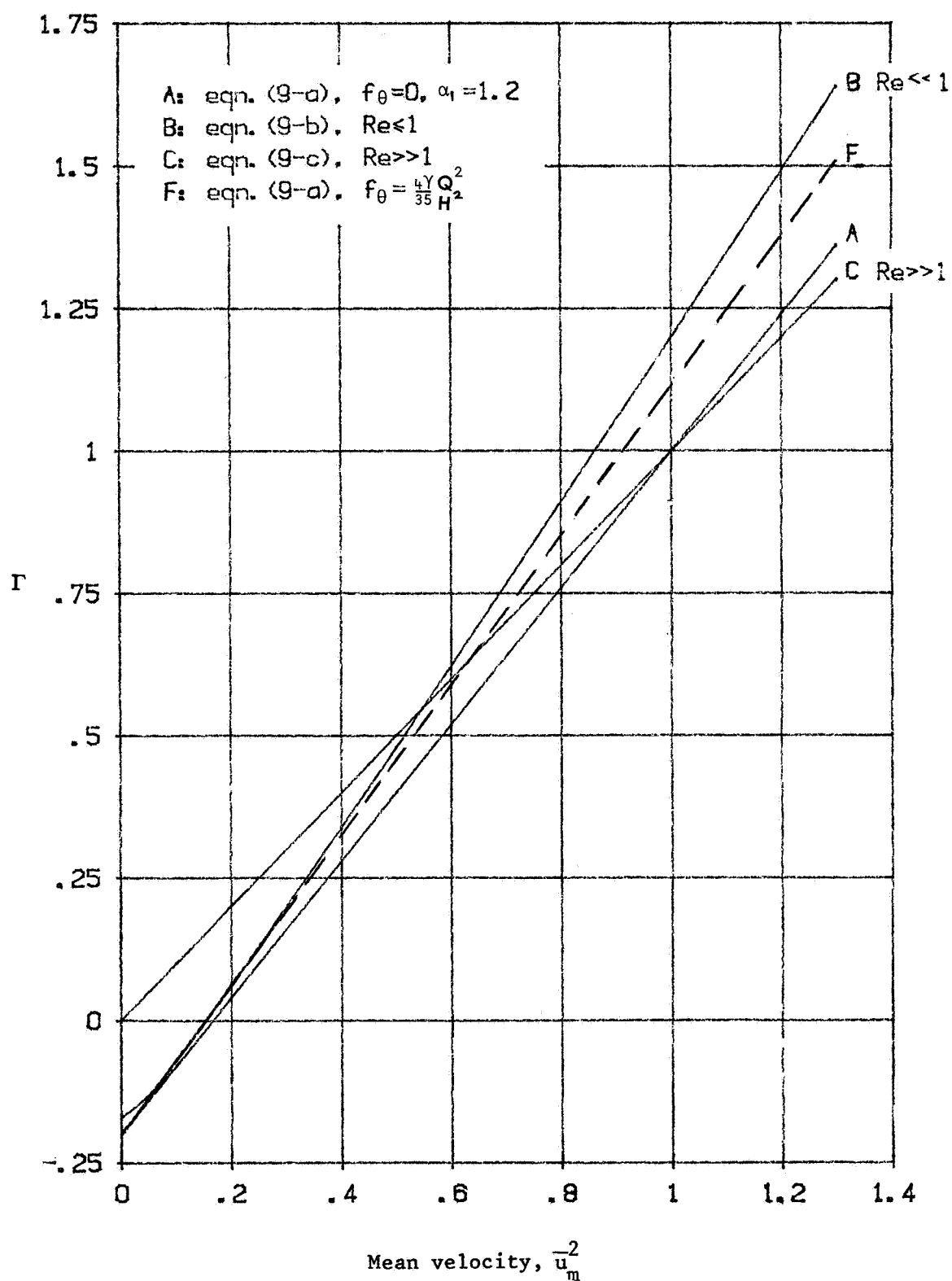
Figure 2. – Function $\Gamma(\bar{u}_m^2)$ indicating magnitude of inertia term in pressure equation for infinitely long squeeze film damper.
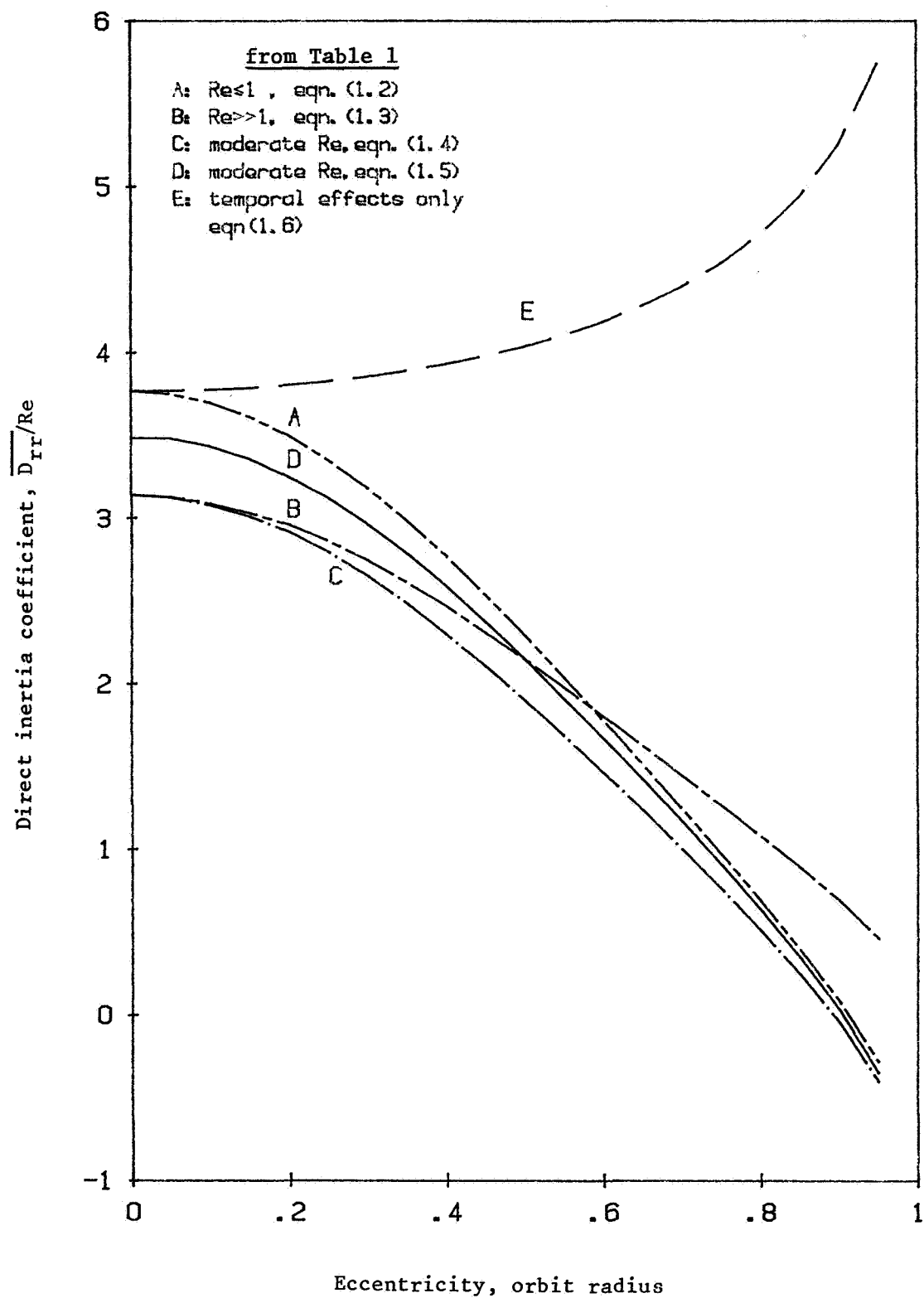
Figure 3. - Direct inertia coefficient $\overline{D_{rr}}$/Re for circular centered orbits as function of eccentricity - long squeeze film damper assumption; laminar flow solution.
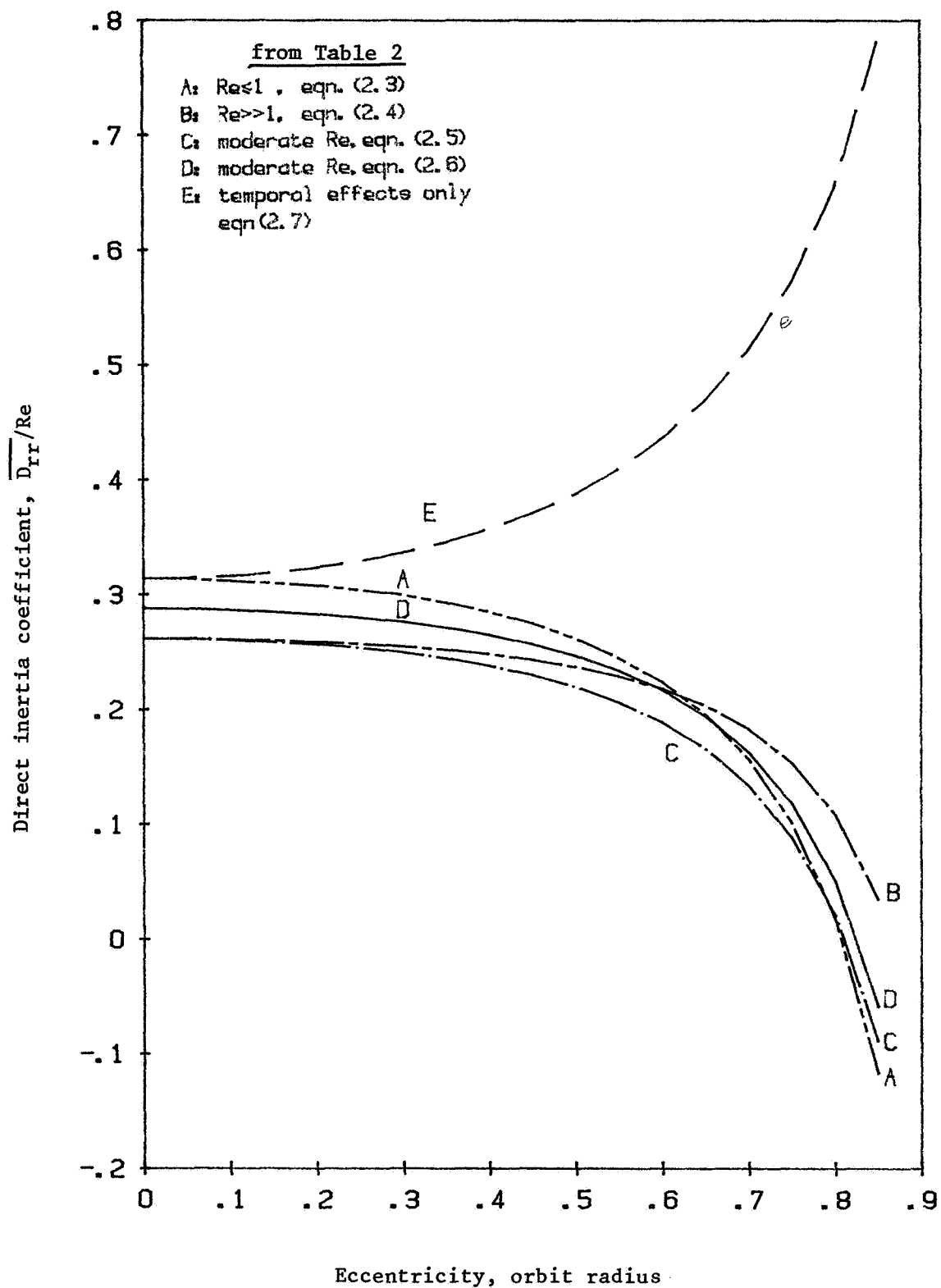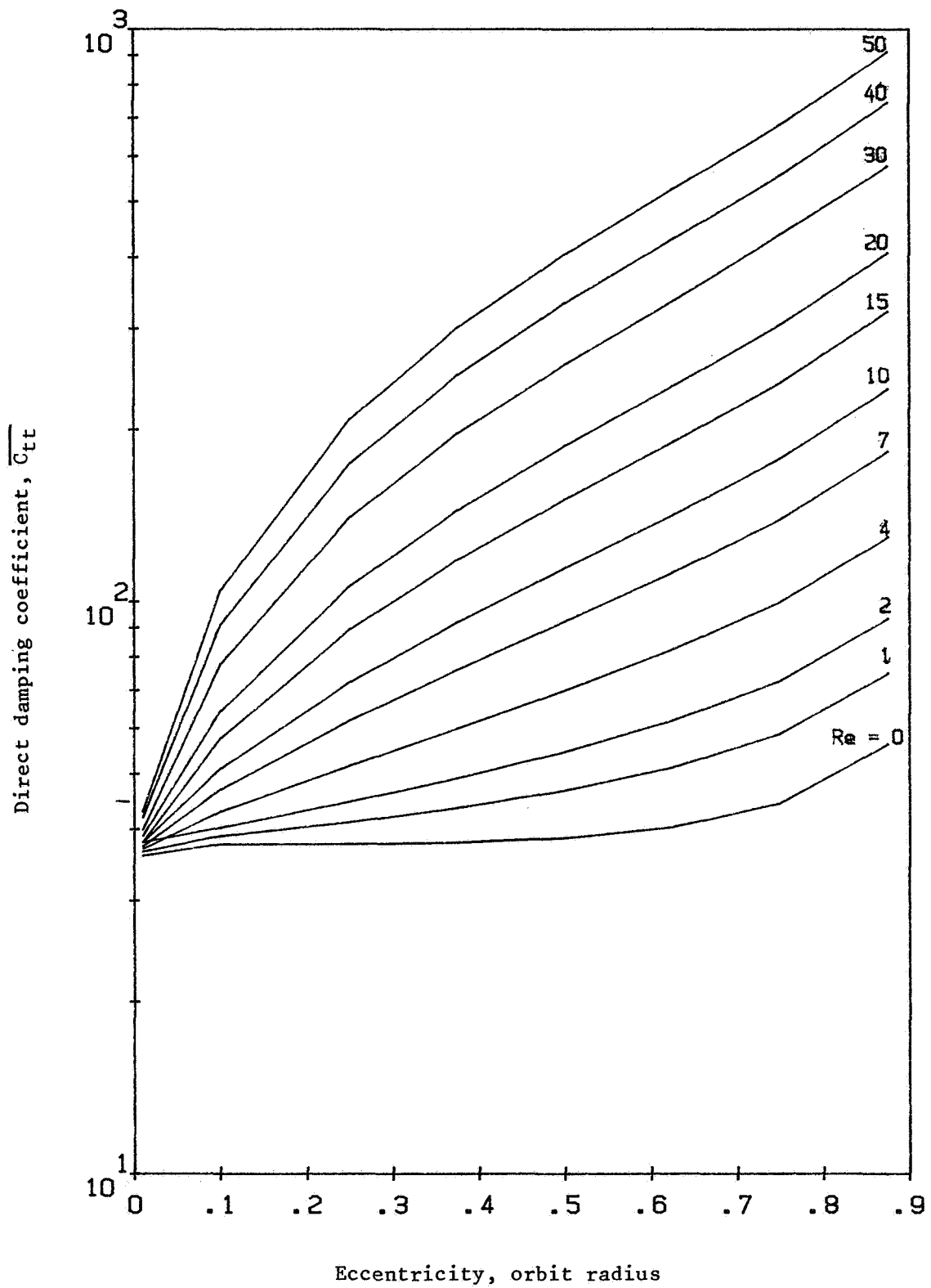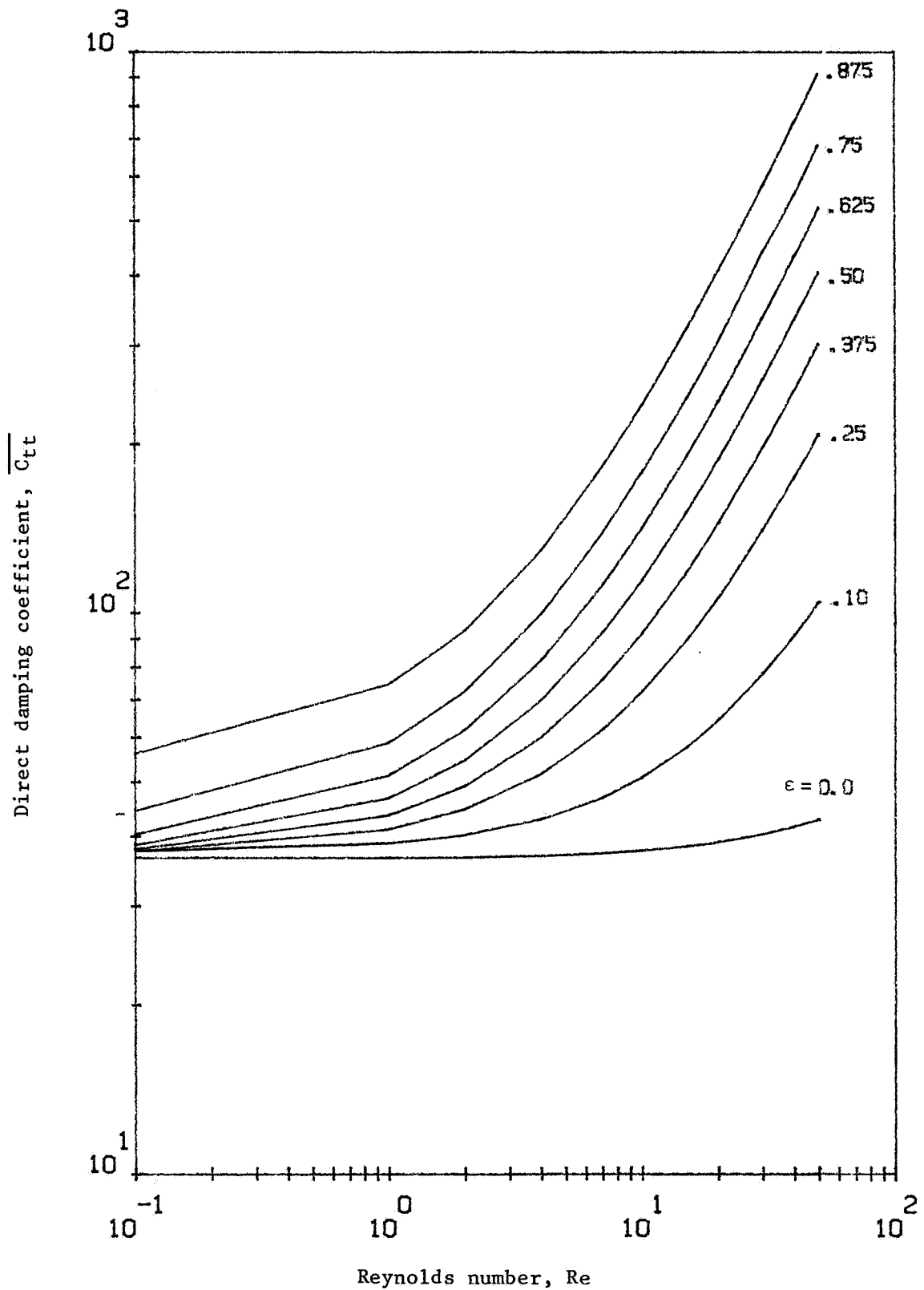
Figure 4. - Direct inertia coefficient $\overline{D_{rr}}$/Re for circular centered orbits as function of eccentricity - short squeeze film damper assumption; laminar flow solution.

Figure 5. - Direct damping coefficient $\overline{D_{tt}}$ for circular centered orbits as function of eccentricity - long squeeze film damper assumption; turbulent motion solution.

Figure 6. – Direct damping coefficient $\overline{C_{tt}}$ for circular centered orbit as function of Reynolds number – long squeeze film damper assumption; turbulent motion solution.
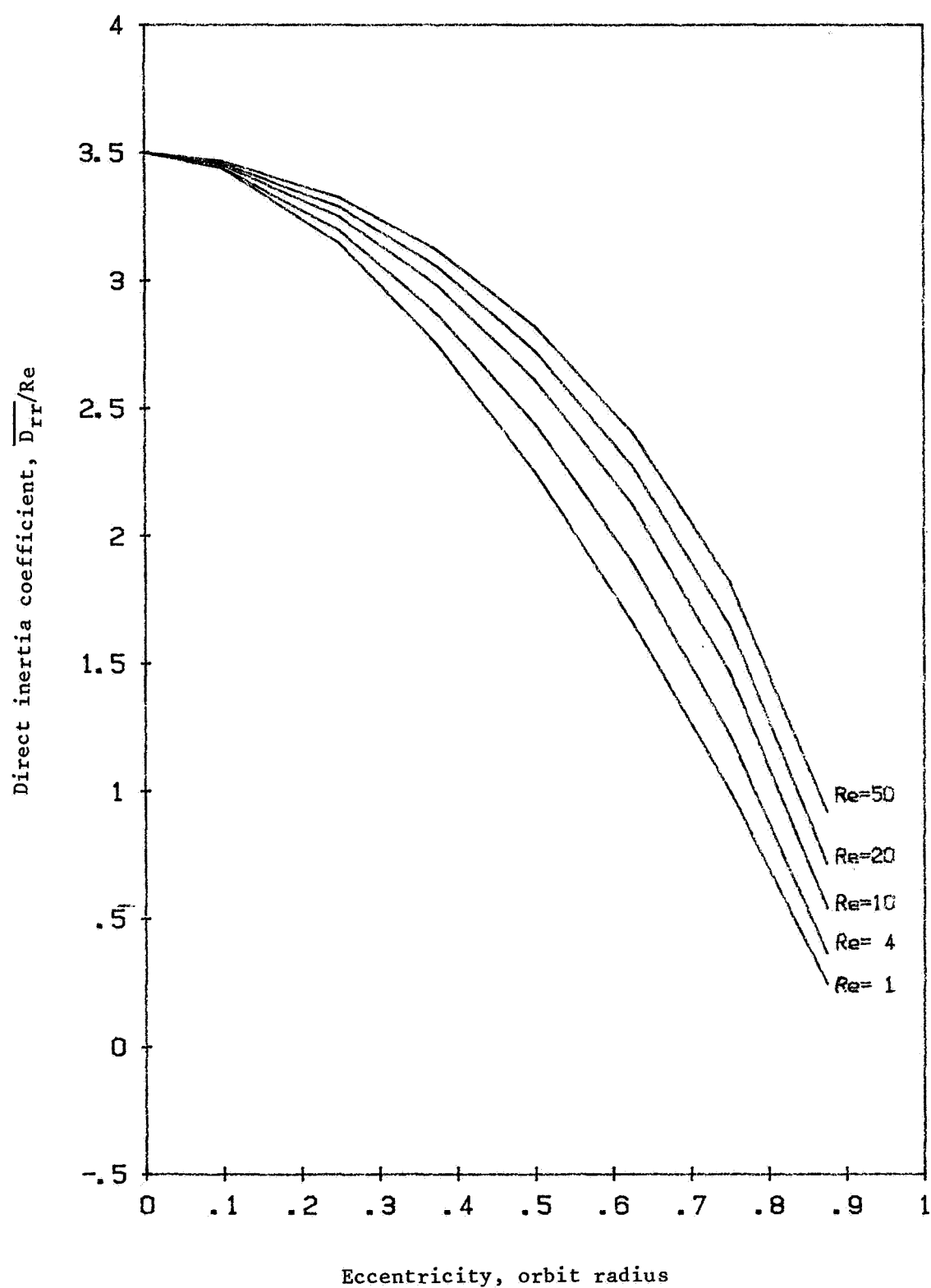
Figure 7. - Direct inertia coefficient $\overline{D_{rr}}$/Re for circular centered orbits as function of eccentricity - long squeeze film damper assumption; turbulent flow solution.
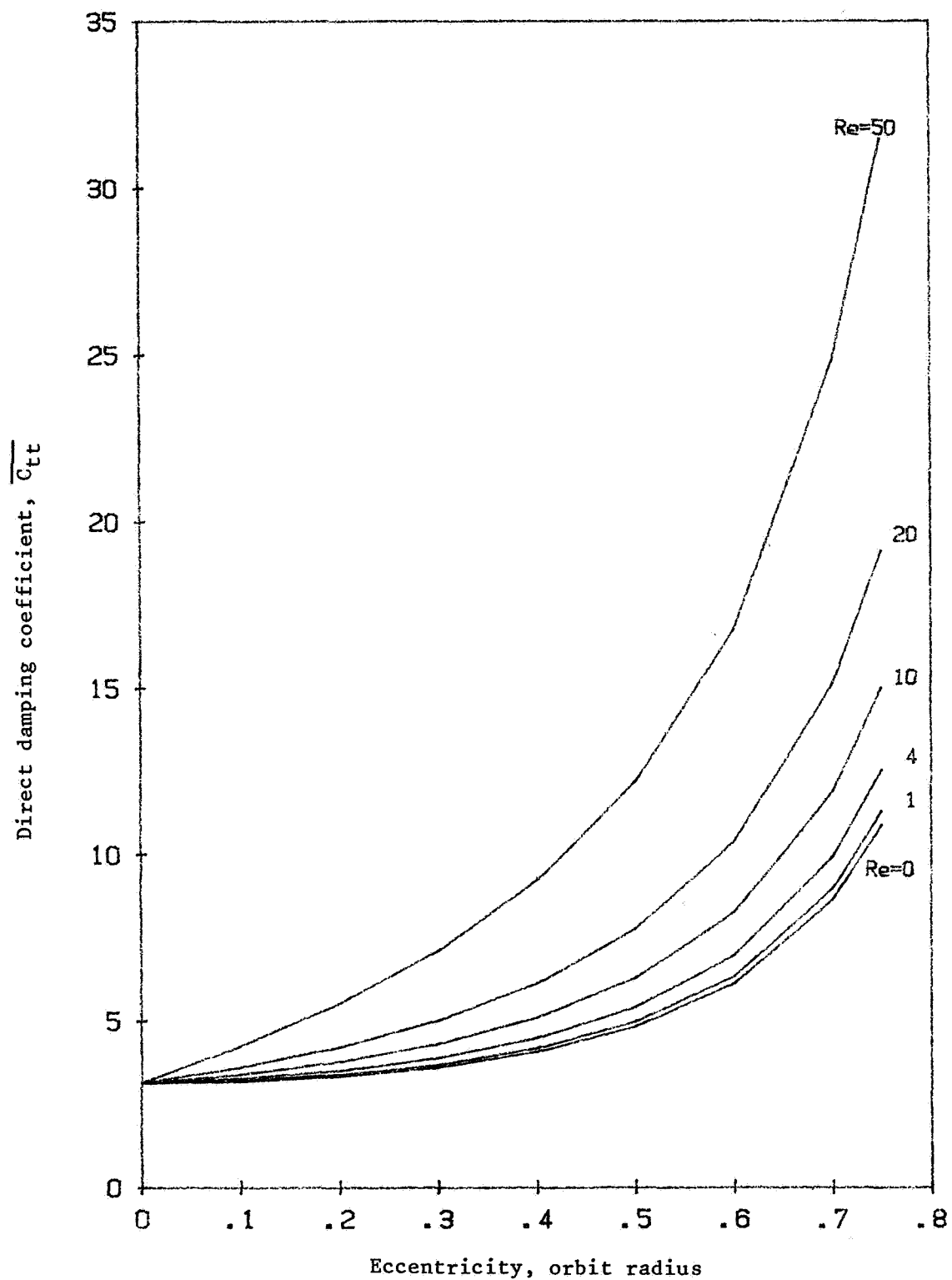
388

Figure 8. - Direct damping coefficient $\overline{C_{tt}}$ for circular centered orbits as function of eccentricity - short squeeze film damper assumption; L/D=0.25; turbulent motion solution.
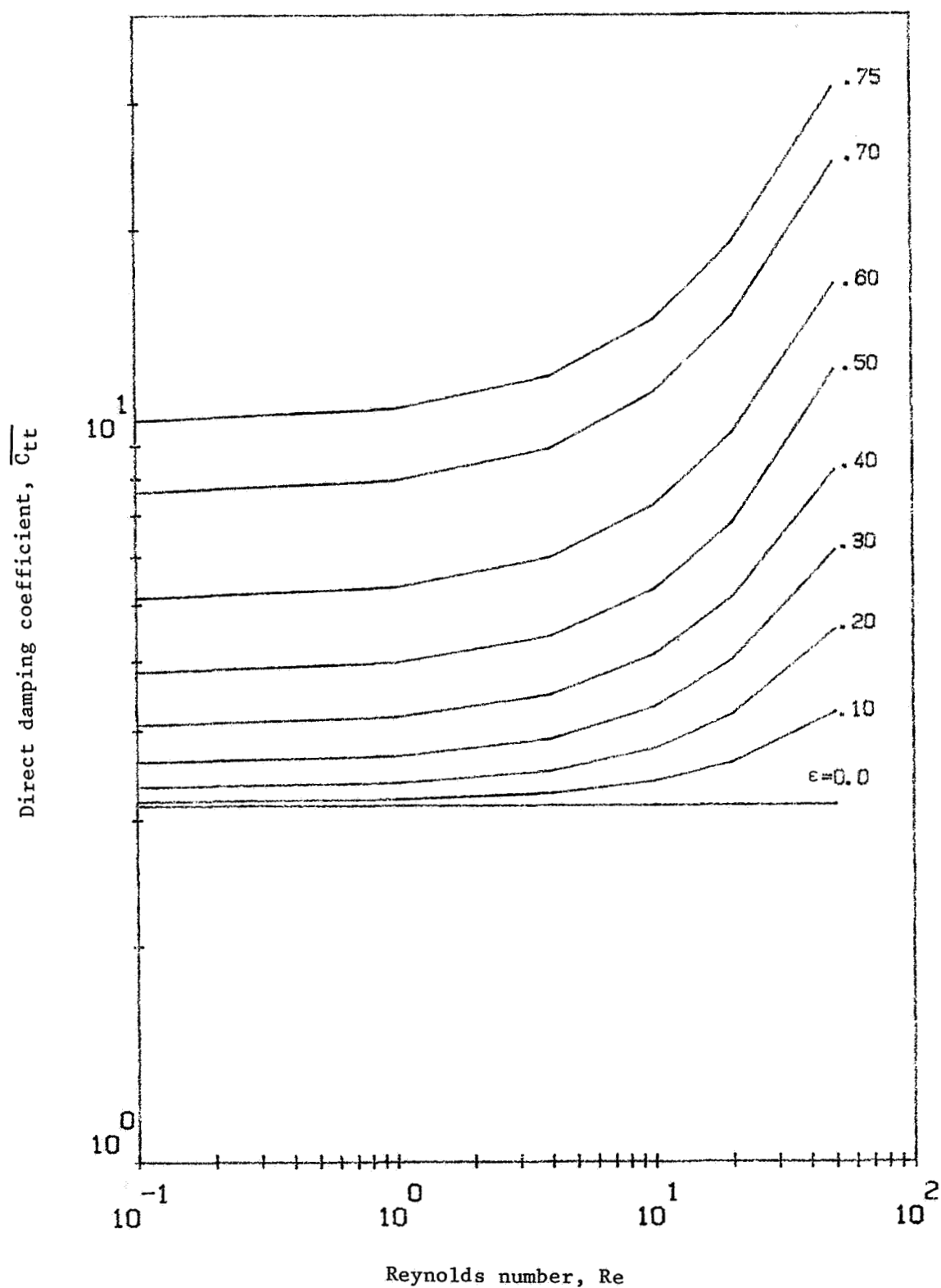
Figure 9. – Direct damping coefficient $\overline{C_{tt}}$ for circular centered orbits as function of Reynolds number – short squeeze film damper assumption; L/D=0.25; turbulent motion solution.